Numerical Methods in Civil Engineering, 9-4 (2025) 62-73

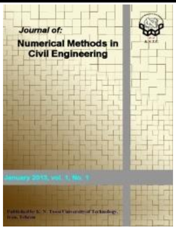

Numerical Methods in Civil Engineering

Journal Homepage: https://nmce.kntu.ac.ir/

Impact of Wave Irregularity on Hydrodynamic Forces Acting on a Vertical Cylinder in the Persian Gulf

Mahdi Saleh*, Rouhollah Amirabadi, Mahdi Sharifi*****

ARTICLE INFO

RESEARCH PAPER

Article history:
Received:
January 2025
Revised:
April 2025
Accepted:
May 2025

Keywords:

Offshore Structure
Dynamic Analysis
Wave Spectrum
Random Wave
Wave Irregularity

Abstract:

The development of marine structures for harnessing natural resources, especially clean energy technologies like offshore wind turbines, is crucial. Waves are a primary design force, significantly impacting the stability and performance of these structures. However, the lack of precise field data and comprehensive wave records poses challenges. This study proposes a novel method to generate accurate artificial wave records efficiently, addressing the limitations of conventional approaches that requires extensive wave data and time-consuming analyses.

Field observations of wave duration and heights in the Persian Gulf were analyzed, and a modified JONSWAP spectrum, tailored to the region, was used to generate random wave records with fewer required waves. The study also examined the impact of wave irregularity on structural forces by comparing forces on a vertical cylinder from the generated wave records and a 100-year return period wave.

Results show that the proposed method achieves high accuracy while significantly reducing computational effort. It successfully identifies spectral peaks and generates reliable wave records using only 50 waves, reducing engineering time by up to 90% while maintaining 97.1% accuracy. The study also introduces a relationship to estimate wave duration based on field data, proposing a 3-hour duration for 100-year return period waves. The findings highlight the method's effectiveness in improving wave load analysis for marine structures in data-scarce regions like the Persian Gulf, offering a robust framework for future research and design optimization.

1. Introduction

The prediction of wave parameters [1] and understanding the impact of waves on marine structures are essential throughout the design and operational phases of such structures. Due to the varying climatic conditions in different regions, this topic has been extensively studied. These studies have examined both fixed structures, such as offshore platforms, and floating structures, including tension-leg platforms and ships [2-3].

Wave analysis not only crucial for offshore platforms but also plays a significant role in the siting, analysis, and design of various breakwaters [4-5]. Laboratory investigations and field observations have consistently proven indispensable for validating computational models. Furthermore, the availability of historical data on wave characteristics and meteorological conditions in the study area is a fundamental prerequisite for this approach [6]. However, such critical data are often either unavailable in many regions or have been collected only over short periods. To address these limitations, numerous researchers are actively developing numerical and software-based models [7-8-9]. The time-intensive nature of time-history-based load modeling remains a topic of discussion in academic and scientific communities. Given the scarcity and limited access to field observations and wave time-series data in many regions, the development of

** PhD student, Faculty of Civil Engineering, University of Qom, Qom, Iran.*
***Corresponding Author: Associate Professor, Faculty of Civil Engineering, University of Qom, Qom, Iran. Email: r.amirabadi@qom.ac.ir*
**** Assistant Professor, Faculty of Civil Engineering, University of Qom, Qom, Iran.*

https://doi.org/10.61186/NMCE.2501.1083

reliable methods for generating artificial wave records is of paramount importance.

Additionally, some studies have proposed that, in the absence of wave data, regional wind data can be utilized to estimate wave characteristics [10]. Regarding wave analysis and standard spectra, Pierson and Moskowitz [11] proposed a formulation based on a theory similar to that of Kitaigorodskii [12], demonstrating that Equation 1 exhibits the highest consistency with experimental data. This relationship is known as the Pierson-Moskowitz spectrum and is expressed as follows:

$$S_\eta(f) = (\alpha g^2/(2\pi)^4) f^{-5}\, exp[-0.74(f_0/f)^4] \quad (1)$$

where α is 0.0081, f_0 is $g(2\pi U_{19.5})^{-1}$, $U_{19.5}$ is the wind speed at 19.5 m above the mean water level and g is the gravitational acceleration. The PM spectrum has been transformed to the following parameterized spectrum using $H_s = 4\sqrt{m_0}$ and $T_P = 1.4\overline{T}$ as [13]:

$$S_\eta(f) = 5/16 {H_s}^2 {f_p}^4 f^{-5}\, exp[-5/4(f_p/f)^4 \quad (2)$$

The Joint North Sea Wave Project (JONSWAP) was formed in 1967 as a partnership with institutions in Germany, the Netherlands, the United Kingdom and the United States. The JONSWAP spectrum was achieved by processing a large number of spectra as follows:

$$S_\eta(f) = \frac{\alpha g^2}{(2\pi)^4} f^{-5}\, exp[-\frac{5}{4}\left(\frac{f_p}{f_m}\right)^4]\gamma^{exp[-\frac{1}{2\sigma^2}\left(\frac{f}{fm}-1\right)^2]} \quad (3)$$

where α is $0.076x^{-0.22}$, x is $gF{U_{10}}^{-2}$, f_m is $(3.5gx^{-0.33})/U_{10}$, σ is $0.07 f \le f_p$ and $0.09 f > f_p$, γ is the peak enhancement coefficient and U_{10} is the wind speed at 10 m above the mean water level. The parameterized spectrum of JONSWAP is as follows:

$$S_\eta(f) = \alpha {H_s}^2 {f_p}^4 f^{-5} \gamma^\beta\, exp[-5/4\left(f_p/f_m\right)^4] \quad (4)$$

where $\alpha \approx \frac{0.0624}{0.230+0.0336\gamma-\left(\frac{0.185}{1.9+\gamma}\right)}$ and $\beta = exp[-\frac{(f-f_p)^2}{2\sigma^2 {f_p}^2}]$.

The values and parameters in this equation have been studied in recent years for different climatic conditions and areas and the results of such research are presented in Table 1. The modified JONSWAP spectrum is presented in Figure 1.

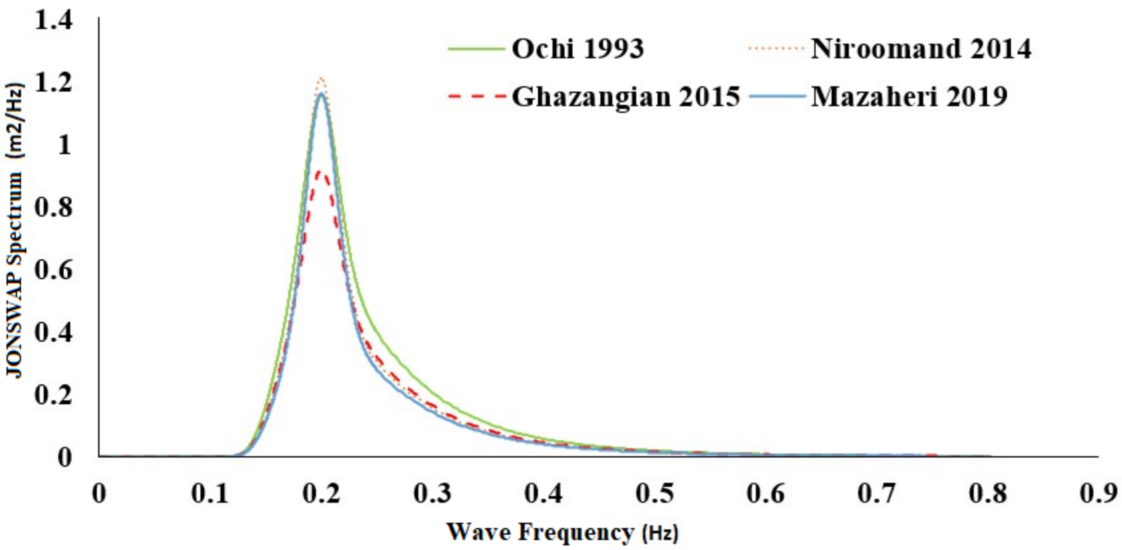

Fig. 1: Modified JONSWAP spectrum (Hs=1.2 m, fp=0.20 Hz) [14-15-16-17]

After determining the suitable spectrum of the area, the optimal wave record extraction method should be used an irregular wave consists of the superposition of multiple regular wave components. One challenge lies in generating an accurate irregular wave record using a minimum number of regular waves. This has been previously covered in several articles, including the work of Journee and Massie (2001) as:

$$\eta(t) = \sum_{n=1}^{N} \eta_a (k_n x - \omega_n t + \varepsilon_n) \quad (5)$$

where η_a is the wave amplitude component (m), ω_n is the circular frequency component (rad/s), k_n is the wave number component (rad/m) and ε_n is the random phase angle component (rad). Variance ${\sigma_\eta}^2$ of this signal equals:

$$ {\sigma_\varsigma}^2 = \overline{\varsigma^2} = \frac{1}{N}\sum_{n=1}^{N} {\varsigma_n}^2 = \frac{1}{N.\Delta t}\sum_{n=1}^{N} {\varsigma_n}^2 . \Delta t = \frac{1}{\tau}\int_0^\tau \varsigma^2(t). dt = \frac{1}{\tau}\int_0^\tau \left\{\sum_{n=1}^{N} \varsigma_{a_n} cos(\omega_n t - k_n x + \varepsilon_n)\right\}^2 . dt = \sum_{n=1}^{N} \frac{1}{2} {\varsigma_{an}}^2 \quad (6)$$

Table 1: Proposed values and relationships for Phillip's constant, peak enhancement factor and narrowness of the peak parameter from previous studies and present study [17]

Authors	Phillip's constant	Peak-enhancement factor	Narrowness parameter
Hasselmann [18]	$0.076(\frac{V_{10}^2}{gd})^{0.22}$	3.3	$\sigma = \begin{cases} 0.07 & f \leq f_p \\ 0.09 & f > f_p \end{cases}$
Ochi and Hubble [19]	0.0023	2.2	-
Ochi [14]	$4.5H_S^2 f_P^4$	$9.5H_S^{0.34} f_P$	-
Young and Verhagen [20]	-	-	0.12
Young [21]	$0.008(\frac{V_{10}}{C_P})^{0.73}$	1.9	0.1
Kumar and Kumar [22]	$0.18H_S^{1.52} T_P^{-3.53} T_{0.2}^{1.34}$	$8.38H_S^{0.57} T_P^{-1.26} T_{0.2}^{0.41}$	-
Mazaheri and Ghaderi [23]	$4.5H_S^2 f_P^4$	$7.5H_S^{0.34} f_P$	-
Feng et al. [24]	$4.069H_S^{2.06} T_P^{-4.24}$	$6.236H_S^{0.12} T_P^{-0.34}$	-
Niroomand et al. [15]	$3.4H_S^2 f_P^4$	1.8-3.8	$\sigma = \begin{cases} 0.12 - 0.19 & f \leq f_p \\ 0.08 - 0.12 & f > f_p \end{cases}$
Mazaheri and Arabzadeh [25]	$1.25H_S^{1.8} f_P^{3.35}$	$5.5H_S^{0.3} f_P^{0.6}$	-
Ghazangian et al. [16]	0.0083	2	-
Mazaheri and Imani [17]	$1.25H_S^{1.93} f_P^{3.78}$	$8.54H_S^{0.3} f_P^{0.7}$	-

Wave amplitude ς_{a_n} can be expressed in a wave spectrum $S_\varsigma(\omega_n)$ defined as:

$$S_\varsigma(\omega_n).\Delta\omega = \sum_{\omega_n}^{\omega_n+\Delta\omega} \frac{1}{2} \varsigma^2{}_{a_n}(\omega) \tag{7}$$

where $\Delta\omega$ is a constant difference between two successive frequencies. Figure 2 shows analysis of a wave record.

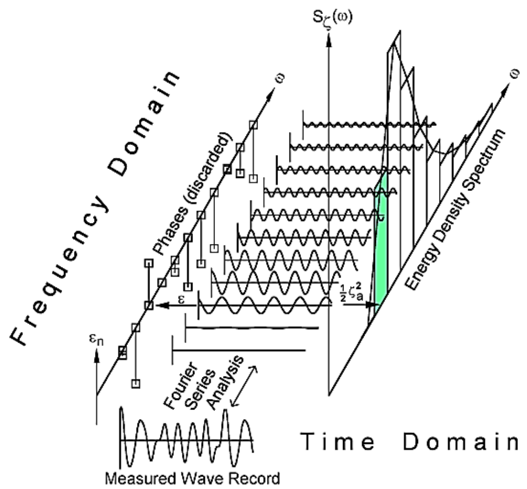

Fig. 2: Wave record analysis [26]

The calculation of wave forces is a critical aspect of research and design in marine structures. Most research efforts have focused on the forces generated by regular waves. Accurate calculation of these forces is essential to ensure the safety and stability of marine structures, as these forces directly influence the design and performance of such structures under varying sea conditions. Further research is needed to investigate the effects of irregular waves, wave spectrum analysis, and real-world scenarios to improve design methodologies. Interest in predicting wave forces has grown due to increased global investment in offshore operations and the move toward deeper waters. Larger structures required in these deeper waters demand faster and more accurate estimations of wave forces.

In this context, Wheeler [27] proposed a method for calculating forces generated by irregular waves, though this method exhibits approximately 36% deviation from measured values. Ishida et al. [28] conducted wave modeling under laboratory conditions to validate a method developed by Morrison et al. However, steep irregular waves exhibit nonlinear characteristics that should not be overlooked. Mes studied the impact of peak wave forces on an offshore platform [29]. This study revealed that using regular wave theory might overestimate the horizontal wave pressure on the deck. Additionally, the maximum deck loading occurs only once during a specific storm event and lasts about two seconds [29]. Gudmestad [30] emphasized the importance of considering both economic and safety design aspects, stating that there is currently no theory capable of reliably predicting the kinematics of irregular waves. This issue is of critical importance for the construction of offshore structures in deep oceans. This study successfully reduced the standard deviation associated with the uncertainty of wave velocity prediction by 72%. Venugopal et al [31]. investigated wave kinematics factors using storm data collected from a jack-up platform in the North Sea. They found that the wave kinematics factor varied between 0.78 and 0.92. When calculating loads for fixed structures, it is essential to use the wave kinematic factors at the peak of the storm [31]. Aggarwal et al. suggested that for large cylinders, the drag force contribution can be neglected. Additionally, the Morrison equation can be applied to large cylinders and provides relatively good agreement with numerical results [32].

In this context, they also investigated the impact of wave breaking location on the monopile foundation of a wind turbine. Waves generated by surge and reflected waves from the cylinder led to an increase in the peak spectral density near the cylinder [33]. Furthermore, in 2017, Young conducted a study proposing various methods for describing ocean waves. In this study, three notable approaches were employed. First, the wave field can be represented by a single periodic wave with a specific height, period, and direction (regular waves). Second, a number of primary wave harmonics can be used to reconstruct non-sinusoidal characteristics (irregular waves). Finally, the water surface can be estimated as the summation of an infinite number of Fourier components. Advancements in measurement capabilities and data evaluation have made full spectral descriptions increasingly common. Yet, the appeal of using a single characteristic, such as height, duration, or direction, remains strong in practical applications. Sayeed et al [35]. stated that one of the primary objectives of studies should be to explore the feasibility of using regular wave data instead of irregular wave data. Additionally, this study examined whether the principle of superposition could also be applied to determine the statistics of irregular wave motions. Ultimately, the results showed that the force data generated using the superposition principle and directly recorded force data exhibited similar trends [35].

associated high computational costs and person-hours required for the project pose a significant challenge. To address this issue, this study introduces an appropriate classification method, which not only significantly reduces the number of waves but also achieves acceptable accuracy compared to previous methods. In this approach,

By reviewing the existing literature and historical background on the calculation and application of wave loads in the form of time series, the primary concern and objective is to generate such data with an appropriate number of time steps while maintaining accuracy. Conventional methods often require a significant number of time steps, leading to time-consuming analyses. Therefore, the main goal of this research is to propose a novel method for the optimal generation of wave time-series data. To achieve this, field observations of wave duration with varying heights in the Persian Gulf were first evaluated. Subsequently, a novel approach was introduced to generate random wave records with a substantially reduced number of required waves, utilizing a modified JONSWAP spectrum tailored to the Persian Gulf region. Finally, the impact of wave irregularity on the structural forces was investigated. For this purpose, a comparison was made between the force exerted on a vertical cylinder by the randomly generated wave record using the proposed method and the force resulting from a 100-year return period wave. The details of this study are presented in the following sections.

2. Modeling and Methodology

The present study is divided into three distinct sections. In the first section, a method and theoretical framework are presented to estimate the minimum number of waves required to generate an irregular wave record. In the second section, the minimum wave duration in the Persian Gulf region was comprehensively examined. In the final section, a detailed comparison has been made between the force exerted by regular waves, which constitute an irregular wave, and the force resulting from a 100-year return period wave, in accordance with Equation 8.

$$(F_1 + F_2 + \dots + F_n)/F_{MAX} \quad (8)$$

2.1 Investigation of the Required Number of Waves

In numerous studies, the minimum number of waves required to generate an irregular wave record has been investigated. For instance, the DNV-RP-C205 standard recommends a minimum of 1000 waves for simulating a short-term sea state [36]. The accurate identification of the peak spectral frequency is cited as one of the primary reasons for the high number of waves specified in such standards. Although increasing the number of waves can enable precise calculations, the

leveraging the narrow-banded nature of the JONSWAP spectrum, it is divided as illustrated in Figure 3. This classification is introduced to optimize the estimation process, reduce costs, and maintain computational accuracy.

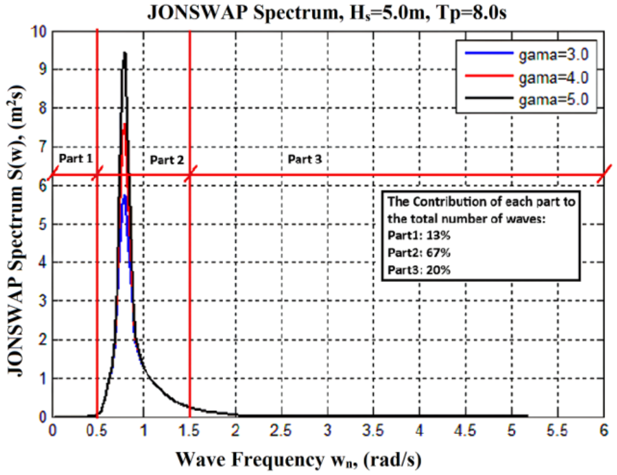

Fig. 3: Suggested spectrum division where *n* is the total number of waves: (part 1) 2*n*/15; (part 2) 10*n*/15; (part 3) 3*n*/15

Initially, the division process was initiated by plotting the spectrum using 1000 waves to determine the main energy range. Then, the division was refined and finalized through an iterative trial-and-error approach to achieve higher precision.

Given the concentration of energy within a narrow frequency range, this study proposes a division of the spectrum. The spectrum is divided into three frequency domains, with the primary data generated in the main energy range of the spectrum. A sensitivity analysis was conducted to evaluate the relationship between the number of waves and accuracy. After thorough examination and trial-and-error, the spectrum was divided into three parts as follows: **Section 1: 2n/15**, **Section 2: 10n/15**, and **Section 3: 3n/15**, where **n** represents the total number of waves.

Wave energy concentration within narrow frequency bands improves spectral peak identification precision. For this reason, in line with additional investigations the removal of parts 1 and 3 were also investigated (Figure 4), the results show:

- With all sections (proposed method): Wave height (H_{ch}) = 4.97 m (nearly matches the target 5 m)
- Without Sections 1-3: H_{ch} drops to 4.8 m
- The error increases for smaller γ values

Since the proposed method focuses on reducing wave count while maintaining acceptable accuracy, excessive reduction in wave numbers may compromise calculation precision. Therefore, removing these sections is not recommended.

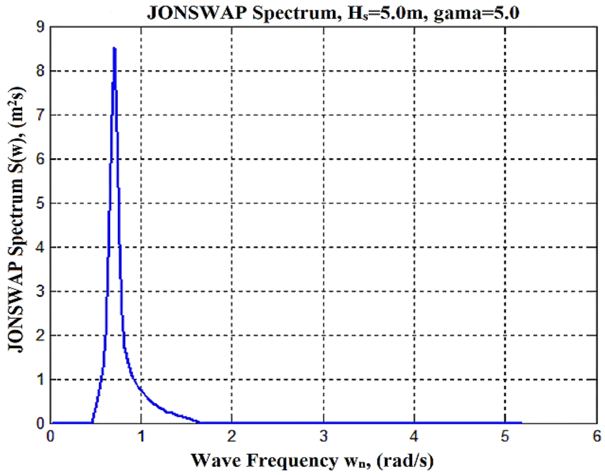

Fig. 4: Spectrum Assuming Removal of parts 1 and 3

To validate the implemented code, both approaches (with and without the proposed classification) are compared against the spectrum provided in the DNV-RP-C205 standard, assuming 1000 waves. This comparison is illustrated in Figure 5. It helps evaluate the efficiency and accuracy of the different methods in identifying spectral peaks and generating random wave records. For a thorough comparative analysis between the proposed method and conventional approaches, Figure 6 systematically examines the following aspects:

1. High-Resolution Reference (N=1000):
   - 0-5 Hz range divided into 1000 equal segments (df = 0.005 Hz)
   - Complies with DNV-RP-C205 requirements for benchmark spectra
2. Conventional Equal Division:
   - 50 uniform segments (df = 0.1 Hz)
   - Represents standard engineering practice
3. Optimized Proposed Division:
   - 50 non-uniform segments
   - Adaptive df based on energy concentration (per Figure 3)
   - The proposed division method optimizes computational efficiency while maintaining spectral accuracy

The results in this section demonstrate that the proposed method exhibits high accuracy in identifying spectral peaks and is capable of generating acceptable random wave records. The maximum deviation of the plotted spectrum (with and without the proposed classification) compared to the spectrum suggested in the DNV-RP-C205 standard, assuming 1000 waves, is presented in Table 2 and Figure 6.

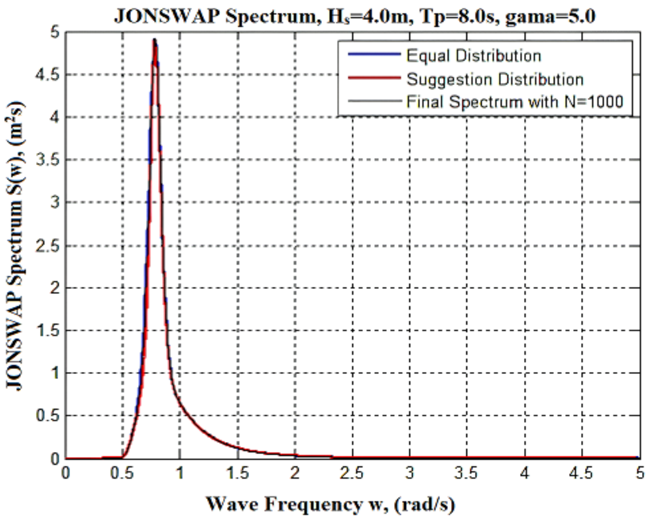

Fig. 5: Spectral division schemes compared: (a) N=1000 reference, (b) Equal 50-parts division, (c) Proposed optimized 50-parts division (per Fig. 3)

This comparison provides a detailed analysis of the differences and the efficiency of the various methods in identifying spectral maxima.

The results indicate that, by using the proposed division, the spectral peak can be accurately identified with just 50 waves. These findings highlight the efficiency of the proposed method and its contribution to improving accuracy in hydrodynamic analyses.

Table 2: Deviation from real spectrum peak

NUMBER OF WAVES	EQUAL DIVISION	PROPOSED DIVISION
25	62%	11%
50	19.6%	2.9%
100	1.8%	0.05%
150	0.5%	<0.01%
250	<0.3%	<0.01%
500	<0.01%	<0.01%
1000	<0.01%	<0.01%

On the other hand, generating a stationary and ergodic random wave record using conventional methods typically requires a minimum of 500 waves. However, by employing the proposed classification, this objective can be achieved with only 50 waves. Figure 7 illustrates the wave records generated using different numbers of waves.

2.2 Calculation of Wave Duration

One of the most critical aspects of generating an artificial wave record is the accurate estimation of its duration. This issue is particularly significant in fatigue analysis and requires careful consideration. Since real-world data from field measurements are often unavailable in many regions, this challenge is addressed in the present study.

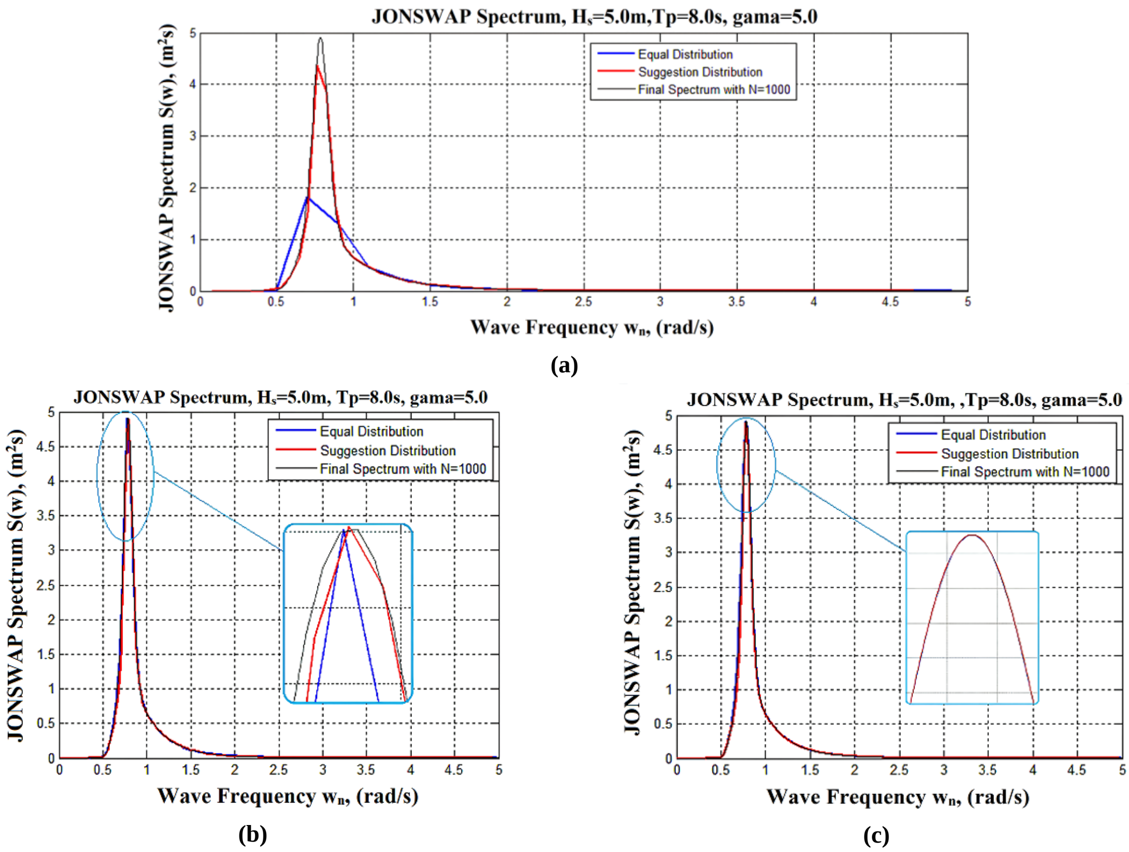

Fig. 6: JONSWAP spectra for H_s = 4.0 m and T_p = 8.0 s with different numbers of waves (a) n=25, (b) n=150, (c) n=1000

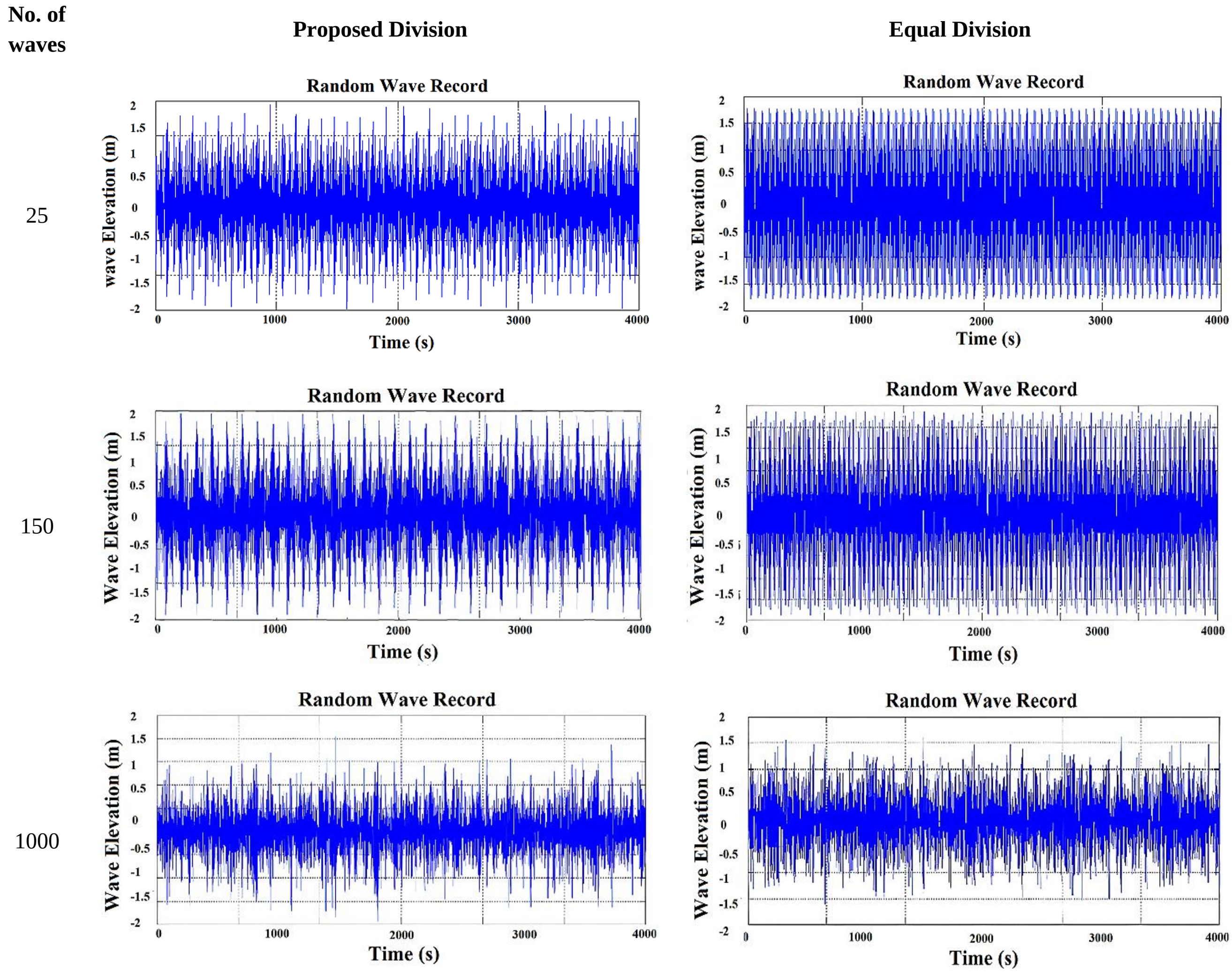

Fig. 7: Wave records generated for different numbers of waves with equal and proposed divisions

In this study, the wave duration was initially calculated using field observations in the Persian Gulf, specifically in the South Pars region, based on data provided in the Gelen report [37]. The approximate location of the field observations is 52°05'59" E and 26°46'20" N. These data include a report on oceanographic conditions influencing the design and operation of the South Pars Gas Field development project. Finally, the statistical validation of the generated wave record was performed using the modified spectrum proposed by Mazahari and Imani [17], which is consistent with the conditions of the Persian Gulf, as well as the approach introduced by Kamphuis [38]. This statistical validation helps assess the accuracy of the generated record and its alignment with real-world conditions.

The collected data from the study area were categorized by season and by wave heights greater than 1, 2, and 3 meters, as presented in Table 3. This categorization facilitates a detailed analysis of wave behavior across different seasons of the year.

It is important to note that a generated wave record can only be a comprehensive representation of the sea state if it includes all the statistical characteristics associated with the waves in that state. For this purpose, the artificial wave record generated was validated against the actual conditions of the region. Table 4 presents the characteristics of waves with a 100-year return period in different directions, based on field observations [37].

Based on the data provided in Table 4, the maximum significant wave height (Hs) is 6.6 meters in the northwest direction. Therefore, in this study, this height has been considered as the basis for calculations. Figure 8 illustrates the modified JONSWAP spectrum for the Persian Gulf, based on the coefficients provided by Mazahari and Imani [17]. It is also worth noting that the accuracy of this spectrum has been verified and confirmed against the referenced study.

Table 3: Average seasonal duration of storms (from field observations [37])

	JANUARY - MARCH			**APRIL - JUNE**			**JULY - SEPTEMBER**			**OCTOBER - DECEMBER**		
	Duration (Hours)			**Duration (Hours)**			**Duration (Hours)**			**Duration (Hours)**		
	H>1	**H>2**	**H>3**	**H>1**	**H>2**	**H>3**	**H>1**	**H>2**	**H>3**	**H>1**	**H>2**	**H>3**
	250	85	30	220	76	24	180	55	8	200	66	12
	205	71	23	180	62	16	145	38	5	160	49	8
	165	59	18	146	49	10	115	24		130	35	6
	130	48	13	117	37		90	12		103	23	
	102	38	9	93	27		71			80	14	
	79	29	6	73	19		54			62	8	
	62	22		57	13		40			47		
	50	17		45	9		30			36		
	41	14		36	6		22			28		
	34	12		29			17			22		
	28	10		24			14			18		
	23	8		20			12			15		
	19	7		17			10			13		
	16	6		15			8			11		
	14			13			7			10		
	12			11			6			9		
	11			10						8		
	10			9						7		
	9			8						6		
	8			7								
	7			6								
	6			6								
	6											
Total Hours Per Season	1287	426	99	1142	298	50	821	129	13	965	195	26
Total Number of Occurences	23	14	6	22	9	3	16	4	2	19	6	3
Overall Average Duration (Hours)	56	30	17	52	33	17	51	32	7	51	33	9

Table 4: 100-year directional maximum and significant wave characteristics [37]

	North		**North East**		**East**		**Southeast**		**South**		**Southwest**		**West**		**Northwest**	
	Max	**Sig**	**Max**	**Sig**	**Max**	**Sig**	**Max**	**Sig**	**Max**	**Sig**	**Max**	**Sig**	**Max**	**Sig**	**Max**	**Sig**
Wave Height (M)	9.7	5.2	8.8	4.8	10.8	5.8	11.6	6.2	10.2	5.5	8.8	4.7	10.8	5.8	12.2	6.6
Wave Period (S)	10.0	9.0	9.6	8.6	10.4	9.4	10.8	9.8	10.2	9.2	9.5	8.5	10.4	9.4	11.0	10.0

To control the adequacy of the duration of the wave, Initially, a 10-hour random wave record was generated using 50 waves, based on the proposed division method presented in previous sections and the frequency step (d_f) was calculated according to figure 3.
Then, from this record:

- 15 random 1-hour segments were extracted
- 15 random 3-hour segments were extracted

Figure 9 illustrates our randomized segment selection protocol and figure 10 is a sample of generated wave record, where:

- n segments are drawn from the full time series
- Segment lengths vary between 1-3 hours
- Spatial overlap <15% to ensure independence

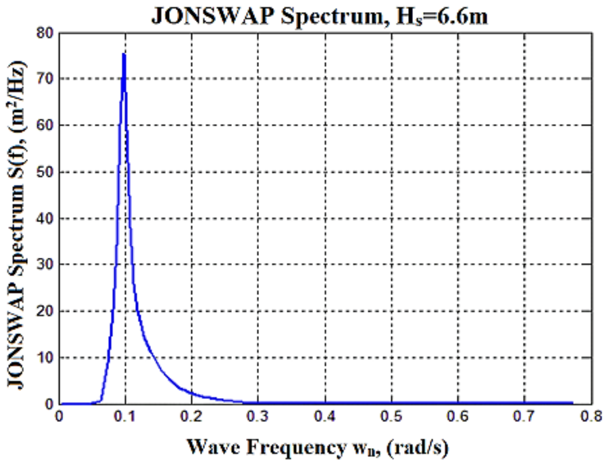

Fig. 8: Modified JONSWAP spectrum using parameters from Mazaheri and Imani [17]

A comparative analysis of the water surface profiles of these extracted records was performed.

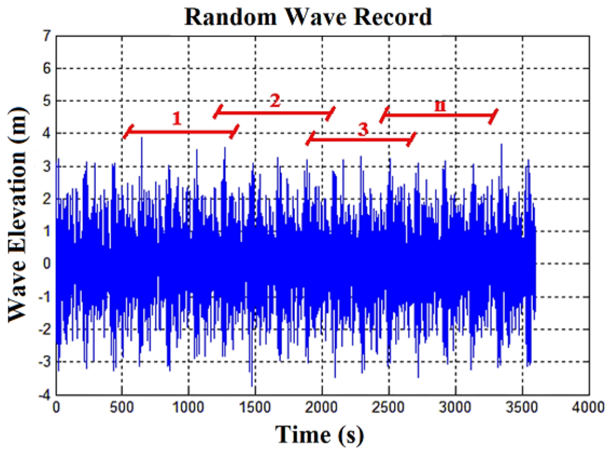

Fig. 9: Example of random segment selection (red lines) from continuous wave data

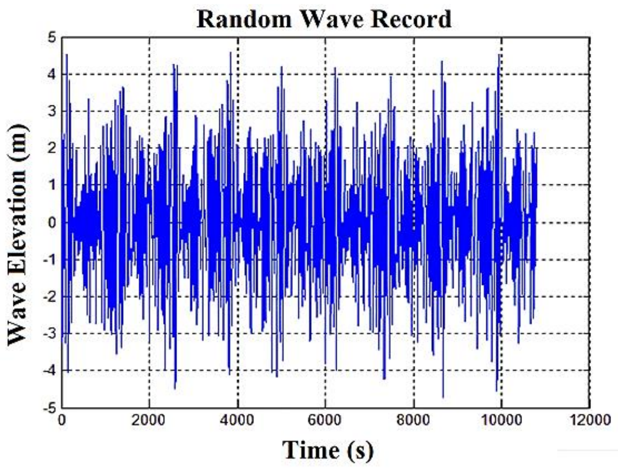

Fig. 10: Random 3-h wave record generated using proposed spectrum

After conducting the relevant analyses, the maximum variance difference among the 15 selected 1-hour records was reported to be approximately 3%. Subsequently, 15 random 3-hour segments were extracted from the existing record, and the analyses revealed that the maximum variance difference among these segments was about 0.3%. Therefore, despite the acceptable accuracy of the 1-hour record, the 3-hour record was chosen as the basis for further calculations in this study (In accordance with the Glenn Report's recommendation [37].

2.3 Calculation of the Ratio of Forces from Generated artificial Waves to Maximum Force

In this section, the ratio of forces generated by artificial waves to the maximum force is calculated. Initially, the force exerted by each regular wave on the vertical cylinder was calculated using the Morrison equation. This equation (Equation 9), as presented in the API-RP2A standard [39], consists of both linear and nonlinear components:

$$F = F_D + F_I = C_D \frac{w}{2g} AU|U| + C_m \frac{w}{g} V \frac{\delta U}{\delta t} \tag{9}$$

where F is the hydrodynamic force, F_D is the drag force, and F_I is the inertial force. Numerical modeling in this study was performed using SAP2000 software [40]. It is worth noting that this model was validated against the numerical example provided by Dawson [41].

In previous sections, it was demonstrated that the proposed method can generate an artificial random wave record consistent with the actual conditions of the Persian Gulf using 50 regular waves. In this stage, based on the principle of superposition, the forces exerted by each regular wave on the vertical cylinder were calculated and aggregated. The principle of superposition is only applicable when both components of the Morrison equation (Equation 9) are linear and does not hold for nonlinear relationships. Therefore, this principle can only be applied when the drag force component in this equation can be neglected. According to the numerical modeling and the relationship provided in equation 10 [40], the contribution of the drag force is less than 2% of the total hydrodynamic force.

$$F_m = \sqrt{{F_{Im}}^2 + {F_{Dm}}^2} = F_{Im}\sqrt{1 + (\frac{\mu H}{D})^2} \tag{10}$$

The drag force, inertial force, and total hydrodynamic force for one of the generated waves are presented in Figure 11. It is worth noting that Agarwal et al. [32] also emphasized that the effect of the drag force is negligible for large cylinders and can be disregarded. Therefore, considering the negligible contribution of the drag force, the time history of the force was calculated using the principle of superposition.

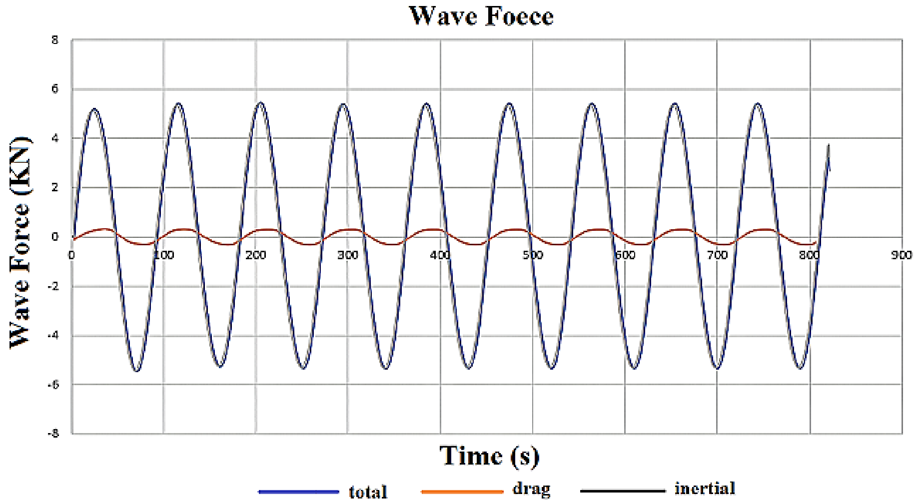

Fig. 11: Sample profile for drag, inertial and total wave forces

API-RP-2A provides kinematic coefficients for different regions [39]. For example, this standard recommends a coefficient of 0.88 for the Gulf of Mexico. Additionally, the specified coefficient for tropical storms ranges from 0.85 to 0.95, while for extratropical storms, it ranges from 0.95 to 1.00. In this study, this coefficient was calculated for wave forces in the Persian Gulf based on the generated random wave record. Figure 12 presents a time history of the generated force.

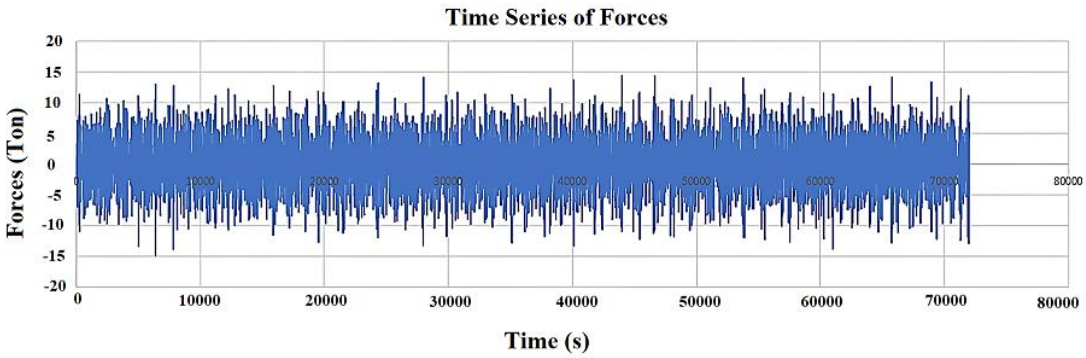

Fig. 12. Time series of forces

Initially, 10 random time history force records were generated, and subsequently compared with the force resulting from the maximum wave height (H_{max}). The time-history force record was generated by superimposing regular wave components, each assigned a random phase shift. This phase variation replicates real-world wave interactions and ensures accurate simulation of irregular wave conditions. The results of this modeling indicate that the ratio of the forces generated by the artificial waves to the force from the maximum wave height varies between 0.77 and 0.9. Additionally, this modeling was performed for waves with heights $H_{0.01}$ and $H_{0.1}$, with the corresponding results presented in Table 5.

Table 5: Modeling results

Wave forces for different heights	Ratio
$(F_1 + F_2 + \ldots + F_n)/F_{MAX}$	0.77 to 0.9
$(F_1 + F_2 + \ldots + F_n)/F_{0.01}$	0.81 to 0.93
$(F_1 + F_2 + \ldots + F_n)/F_{0.1}$	1.19 to 1.38

4. Conclusions

A critical challenge in marine structural analysis and design is the scarcity of accurate field measurement data in target regions. To address this, researchers have long sought methods to generate artificial wave records that accurately replicate local wave conditions. This study introduces novel approaches to generate artificial data with significantly fewer wave records while maintaining high accuracy. The proposed methods not only reduce data generation costs and computational time but also deliver results with exceptional reliability.

Field data and previous studies confirm that the JONSWAP spectrum effectively represents wave behavior in the Persian Gulf, bolstering confidence in model-derived results. Given its compatibility with regional environmental conditions and engineering requirements, the modified JONSWAP spectrum (with its narrow frequency band and concentrated wave energy) proves particularly suitable for wave simulation in this region. By strategically segmenting the wave count, the spectral peak can be determined with remarkable precision.

Key Findings:

1. **Wave Count Reduction:**

The proposed method (Section 2.1) reduces the required number of waves from conventional benchmarks (1,000 waves) to just **50 waves** while achieving:

- **97.1% accuracy** in spectral peak identification (Table 2).
- **99% consistency** between the calculated significant wave height (*Hch*) and the original benchmark (*Hs*), as validated in Section 2.1.
- **Superior computational efficiency**, maintaining <3% error in load calculations.

2. **Irregular Wave Impact:**

The ratio of irregularly generated waves to maximum wave force was found to range between **0.77 and 0.9**, with consistent results for *H0.01* and *H0.1* wave heights (Table 5).

These findings demonstrate the capabilities of the proposed methods for analyzing and designing structures in similar regions and establish a robust basis for future research and studies.

References

[1] zahra hajebi, adel amouzegar, and S. T. O. Naeeni, “Evaluation and comparison of semi-empirical and numerical methods in predicting wave characteristics in the South Caspian Sea,” *Numer. Methods Civ. Eng.*, vol. 9, no. 3, pp. 28–38, 2025, doi: 10.61186/NMCE.2407.1066.

[2] T. S. Sarpkaya, “Wave Forces on Offshore Structures,” *Wave Forces Offshore Struct.*, vol. 9780521896, pp. 1–322, Jan. 2010, doi: 10.1017/CBO9781139195898.

[3] O. . Faltinsen, “Sea Loads on Ships and Offshore Structures. Cambridge University Press,” *Cambridge Univ. Press*, p. 340, 1993.

[4] Y. Zhu, Y. Li, A. Tao, and J. Zhang, “Numerical Modeling of Wave Interaction with Double Curtain-wall Breakwater,” *Procedia Eng.*, vol. 116, no. 1, pp. 1009–1018, Jan. 2015, doi: 10.1016/J.PROENG.2015.08.393.

[5] E. Jafari, M. M. Namin, and P. Badiei, “Numerical simulation of wave interaction with porous structures,” *Appl. Ocean Res.*, vol. 108, p. 102522, Mar. 2021, doi: 10.1016/J.APOR.2020.102522.

[6] F. Zeng, N. Zhang, G. Huang, Q. Gu, and M. He, “Experimental study on dynamic response of a floating offshore wind turbine under various freak wave profiles,” *Mar. Struct.*, 2023, doi: 10.1016/j.marstruc.2022.103362.

[7] W. Bai and R. Eatock Taylor, “Fully nonlinear simulation of wave interaction with fixed and floating flared structures,” *Ocean Eng.*, 2009, doi: 10.1016/j.oceaneng.2008.11.003.

[8] Y. Kim, K.-H. Kim, J.-H. Kim, T. Kim, M.-G. Seo, and Y. Kim, “Time-domain analysis of nonlinear motion responses and structural loads on ships and offshore structures: development of WISH programs,” *Int. J. Nav. Archit. Ocean Eng.*, vol. 3, no. 1, pp. 37–52, Mar. 2011, doi: 10.2478/IJNAOE-2013-0044.

[9] C. Jiang, P. Xu, X. Bai, Z. Zhao, O. el Moctar, and G. Zhang, “A review of advances in modeling hydrodynamics and hydroelasticity for very large floating structures,” *Ocean Eng.*, vol. 285, Oct. 2023, doi: 10.1016/J.OCEANENG.2023.115319.

[10] “Manual, S. P. (1984). Department of the Army. US Army Corps of Engineers.”

[11] W. J. Pierson and L. Moskowitz, “A proposed spectral form for fully developed wind seas based on the similarity theory of S. A. Kitaigorodskii,” *J. Geophys. Res.*, vol. 69, no. 24, pp. 5181–5190, Dec. 1964, doi: 10.1029/JZ069I024P05181.

[12] KITAIGORODSKI S. A, “Applications of the theory of similarity to the analysis of wind-generated wave motion as a stochastic process,” *DSRA*, vol. 9, no. 7–10, pp. 398–398, Jul. 1962, doi: 10.1016/0011-7471(62)90050-5.

[13] Z. Liu and P. Frigaard, “Generation and Analysis of Random Waves,” 1999, *Aalborg Universitet*. Accessed: Jan. 06, 2025. [Online]. Available: https://vbn.aau.dk/en/publications/generation-and-analysis-of-random-waves

[14] Ochi MK, “On hurricane-generated seas,” *Ocean wave Meas. Anal.*, 1993.

[15] B. Niroomand, R. Kamalian, M. Soltanpour, and M. R. Allahyar, “STUDY OF THE WAVE SPECTRA IN THE PERSIAN GULF,” *Coast. Eng. Proc.*, 2014, doi: 10.9753/icce.v34.posters.37.

[16] R. Ghazangian, M. Shafieefar, R. Panahi, and M. R. Allahyar, “An appropriate unidirectional wave spectrum model for the Strait of Hormuz,” *J. Mar. Sci. Appl.*, 2015, doi: 10.1007/s11804-015-1313-y.

[17] S. Mazaheri and H. Imani, “Evaluation and modification of JONSWAP spectral parameters in the Persian Gulf considering offshore wave characteristics under storm conditions,” *Ocean Dyn.*, 2019, doi: 10.1007/s10236-019-01265-3.

[18] K. Hasselmann *et al.*, “Measurements of wind-wave growth and swell decay during the joint North Sea wave project (JONSWAP).,” 1973.

[19] M. K. Ochi, M. K. Ochi, and E. N. Hubble, “SIX-PARAMETER WAVE SPECTRA,” *Coast. Eng. Proc.*, vol.

1, no. 15, p. 17, Jan. 1976, doi: 10.9753/icce.v15.17.

[20] I. R. Young and L. A. Verhagen, “Fetch limited spectral evolution in finite depth water,” in *Proceedings of the Coastal Engineering Conference*, 1997. doi: 10.1061/9780784402429.041.

[21] I. R. Young, “Observations of the spectra of hurricane generated waves,” *Ocean Eng.*, 1998, doi: 10.1016/S0029-8018(97)00011-5.

[22] V. Sanil Kumar and K. Ashok Kumar, “Spectral characteristics of high shallow water waves,” *Ocean Eng.*, 2008, doi: 10.1016/j.oceaneng.2008.01.016.

[23] S. Mazaheri and Z. Ghaderi, “Shallow Water Wave Characteristics in Persian Gulf,” *J. Coast. Res. J. Coast. Res.*, 2011.

[24] W. B. Feng, Y. Bin, C. Haijing, and N. Xingye, “Study on wave spectra in south coastal waters of jiangsu,” in *Applied Mechanics and Materials*, 2012. doi: 10.4028/www.scientific.net/AMM.212-213.193.

[25] said mazaheri and ahmad arabzadeh, “Modification of Wave Spectrum Parameters in Persian Gulf by Considering Field Measurements in Northern Waters,” *J. Mar. Eng.*, vol. 11, no. 22, pp. 119–125, 2016, Accessed: Jan. 06, 2025. [Online]. Available: http://marine-eng.ir/article-1-381-en.html

[26] “Introduction in offshore hydromechanics (OT3600),” *TUDelft, Fac. Mar. Technol. Sh. Hydromechanics Lab. Rep. No. 1267-K, Lect. Notes*, 2001.

[27] WHEELER JD, “METHOD FOR CALCULATING FORCES PRODUCED BY IRREGULAR WAVES,” *JPT, J. Pet. Technol.*, 1970, doi: 10.2118/2712-pa.

[28] H. Ishida and Y. Iwagaki, “WAVE FORCES INDUCED BY IRREGULAR WAVES ON A VERTICAL CIRCULAR CYLINDER.,” in *Proceedings of the Coastal Engineering Conference*, 1979. doi: 10.9753/icce.v16.144.

[29] M. J. Mes, “Wave crest forces on offshore platforms using irregular wave theory,” in *Proceedings of the Annual Offshore Technology Conference*, 1990. doi: 10.4043/6410-ms.

[30] O. T. Gudmestad, “Measured and predicted deep water wave kinematics in regular and irregular seas,” *Mar. Struct.*, 1993, doi: 10.1016/0951-8339(93)90009-R.

[31] V. Venugopal, J. Wolfram, and B. T. Linfoot, “Wave kinematics factor in real and simulated storms,” *Ocean Eng.*, 2005, doi: 10.1016/j.oceaneng.2004.07.009.

[32] A. Aggarwal, M. A. Chella, A. Kamath, H. Bihs, and O. A. Arntsen, “Irregular Wave Forces on a Large Vertical Circular Cylinder,” in *Energy Procedia*, 2016. doi: 10.1016/j.egypro.2016.09.223.

[33] A. Aggarwal, M. A. Chella, H. Bihs, and Ø. A. Arntsen, “Numerical study of irregular breaking wave forces on a monopile for offshore wind turbines,” in *Energy Procedia*, 2017. doi: 10.1016/j.egypro.2017.10.347.

[34] I. R. Young, “Regular, Irregular Waves and the Wave Spectrum,” in *Encyclopedia of Maritime and Offshore Engineering*, 2017. doi: 10.1002/9781118476406.emoe078.

[35] T. Sayeed, B. Colbourne, and D. Molyneux, “Experimental and numerical investigation of wave induced forces and motions of partially submerged bodies near a fixed structure in irregular waves,” *Ocean Eng.*, 2018, doi: 10.1016/j.oceaneng.2018.06.020.

[36] D. N. Veritas, “Environmental conditions and environmental loads,” *Dnv*, 2010.

[37] Gelen, “Report On Meteo-Oceanographic Conditions Affecting Design And Operations,” 1993.

[38] J. W. Kamphuis, “Introduction to Coastal Engineering and Management: Third Edition,” in *Advanced Series on Ocean Engineering*, 2020. doi: 10.1142/9789811208003_0001.

[39] API RP 2A-WSD 22nd Ed., *Planning, Designing, and Constructing Fixed Offshore Platforms - Working Stress Design*. 2014.

[40] Computers and Structures, “SAP 2000,” 2017, *V20.0-integrated software for structural analysis and design. Berkeley, CA, USA: Computers and Structures,*.

[41] T. H. Dawson, *Offshore structural engineering*. 1983.